

Supplementary Information

Fe-Al binary nanocomposite filled dialysis membrane tubes (DMT-HFAO): A modified method for predicting phosphate desorption kinetics from aqueous and soil solutions

A. Kassim¹, Abi M. Taddesse^{2*}, D. Nigussie³, Isabel Diaz⁴, R.H. Nejat⁵

¹*Department of Chemistry, Hawassa College of Teacher Education, Ethiopia*

²*Department of Chemistry, Haramaya University, Ethiopia*

³*School of Plant Sciences, Haramaya University, Ethiopia*

⁴*Instituto de Catálisis y Petroleoquímica, CSIC, c/Marie Curie 2, 28049 Madrid, Spain*

⁵*Department of Applied Chemistry, Adama Science and Technology University, Ethiopia*

**Abi M. Taddesse; abi92003@yahoo.com; +251912018750, P.O.Box 138, Dire Dawa, Ethiopia*

Materials and Methods

Preparation of hydrous ferric oxide (HFO)

Hydrous ferric oxide was prepared following a procedure of Freese et al., 1995.¹ In a typical synthesis 200 g of ferric nitrate nonahydrate were dissolved in 2 L of deionized water, and 1 M NaOH was added drop wise until a pH of 7 to 8 was obtained. The suspension was centrifuged, decanted, and re-suspended in deionized water. This procedure was repeated at least two times. Finally, the HFO was re-suspended in deionized water to obtain a volume of 4 L and adjusted to the desired pH with 0.5 M HCl. The HFO suspension was prepared fresh after sometime to avoid crystallization of hematite and goethite, which would make the oxide more difficult to dissolve in acid.

Assessment of possible leakage of sorbents through the dialysis membranes

Both qualitative and quantitative tests were run to evaluate the potential leakage of the nanosorbents through the dialysis membrane tubes. The aqueous suspension of CPS and APS was designated as HFAO and HAFAO respectively. Accordingly, the qualitative test for possible leakage of iron was found to be negative for all the sorbents employed viz., HFAO, HAFAO and HFO. However, the quantitative test by AAS indicated the presence of trace amount of Fe in the external solution only for the amorphous binary oxide system (HAFAO) due to leakage to the external solution after 24 h. This may be attributed to its smaller size.² Assuming negligible leakage of the amorphous binary sorbent, we employed all the three sorbents for the subsequent sorption-desorption experiments.

Table S1: Selected physical and chemical properties of Gununo and Bishoftu soils
Soil samples sites

Parameters	Gununo	Bishoftu
pH (KCl)	3.52	6.8
Bray I P (mg/kg)	3	17
Total P (mg/kg)	228.0	468.0
OC (%)	1.9	1.4
*Exchangeable Al (cmol/kg)	7	0.01
Fe _{ox} (%)	0.128	0.131
Al _{ox} (%)	0.13	0.11
Fe _{DCB} (%)	0.52	0.59
Al _{DCB} (%)	0.02	0.01
% clay	28	15
% silt	16	16
% sand	56	69
Textural class	sandy clay loam	sandy loam

DCB: dithionite- citrate-bicarbonate- extractable; O_x: oxalate extractable.

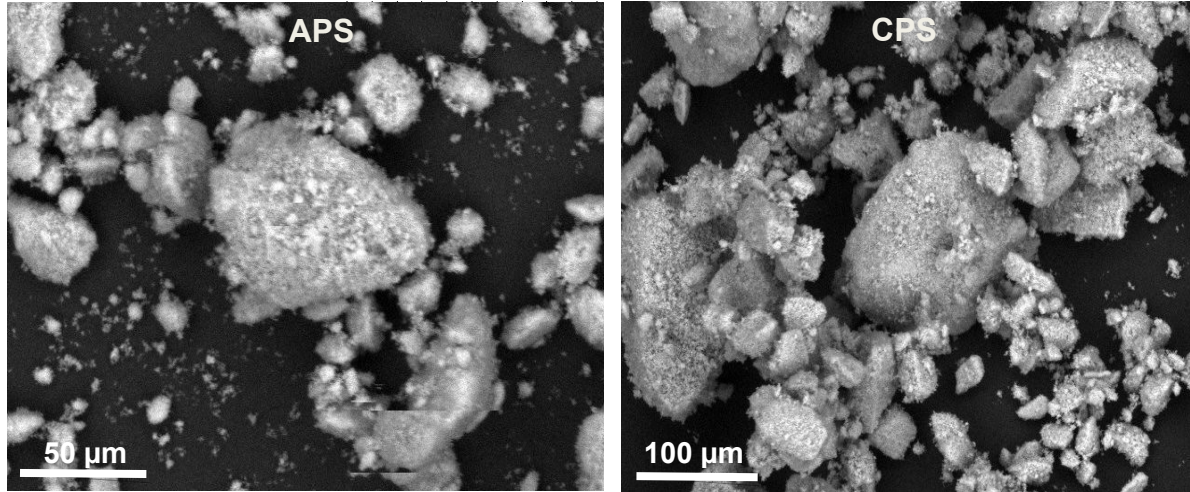


Figure S1. SEM micrographs of amorphous (APS) and crystalline (CPS) Fe-Al binary composite

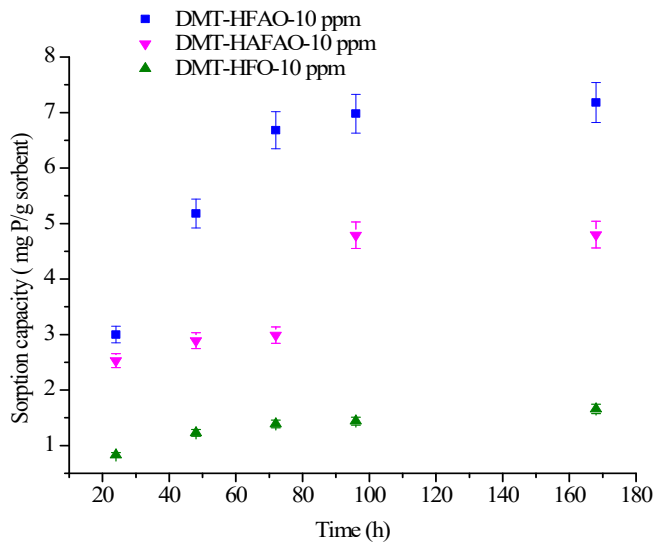
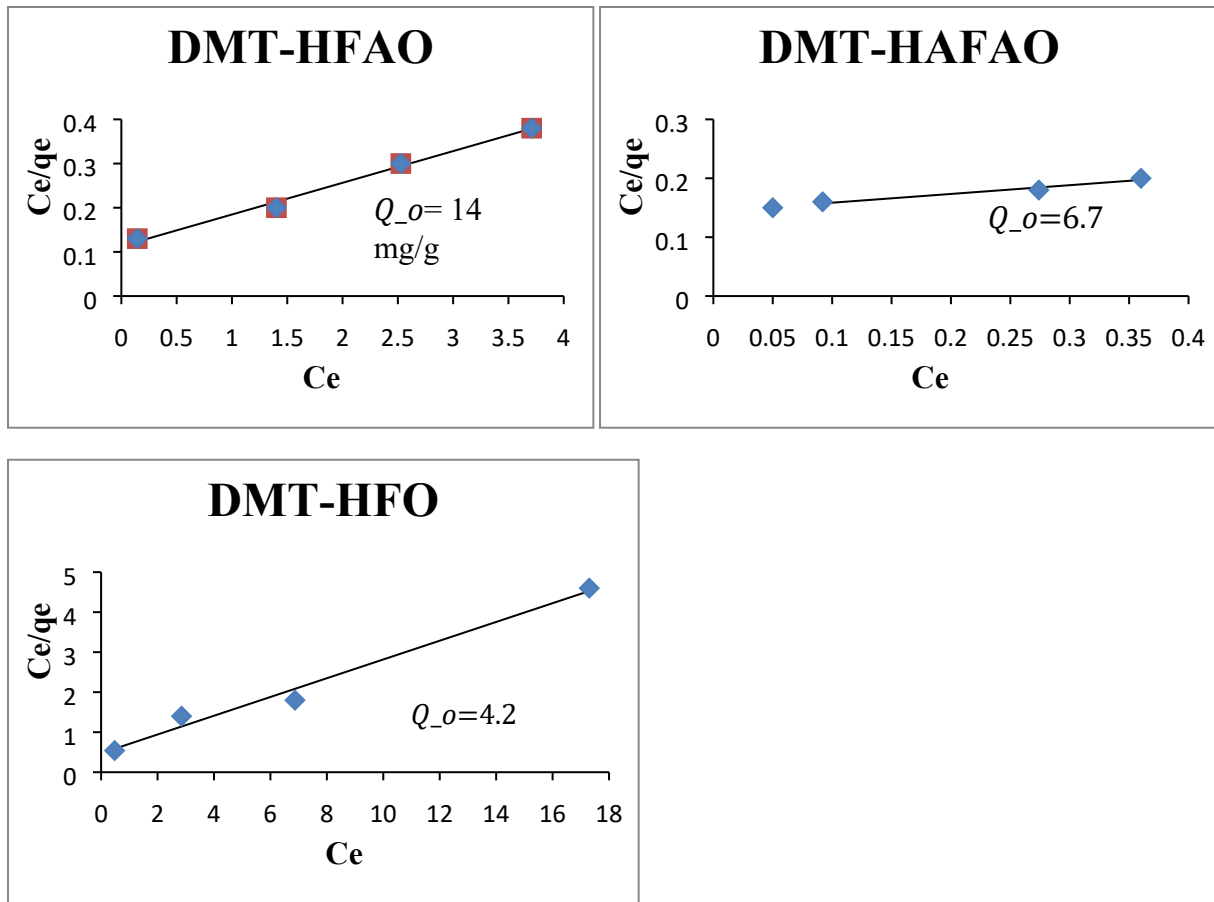


Figure S2: Cumulative P extracted by DMT-sorbent system from 10 ppm P solution. Vertical bars represent error

Table S2. BET specific surface area (m^2/g) of CPS, APS and APS-Fe

Sample	S_{BET}	S_{micro}	S_{ext}	$V_{\text{por(BJH)}}$	Pore volume (cc/g)
CPS	48.7242	0.6884	48.0357	0.013580	0.002404
APS	11.3516	0.4761	10.8755	0.002905	0.005182
APS-Fe	17.1159	0.3442	16.7717	0.004550	0.007907

Langmuir model



Freundlich model

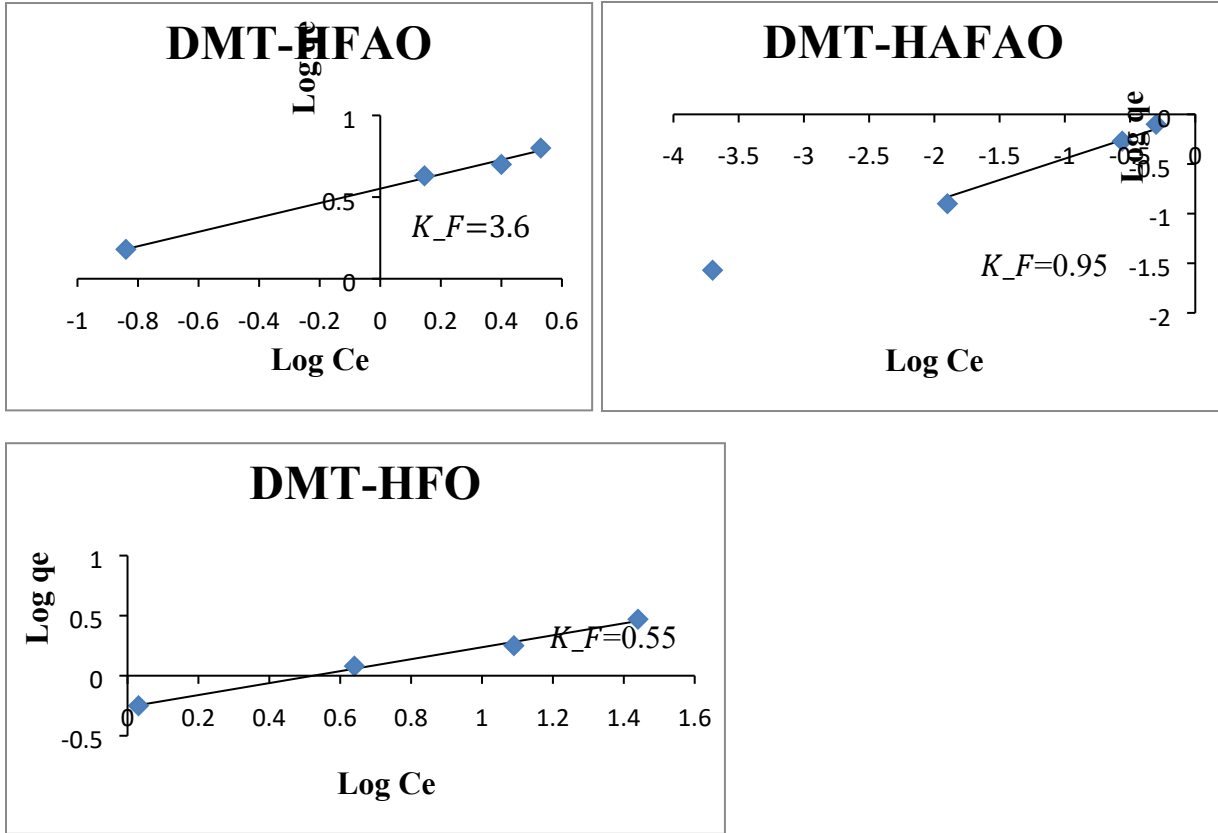


Figure S3: Langmuir and Freundlich models fitted to experimental data generated by DMT-HFO, DMT HFAO and DMT-HAFAO

Kinetic Models

The sorption data were also analyzed using the following kinetics models in linear (a-d) and non-linear form (e).

a. *First order rate law,*

$$\ln C_t = \ln C_0 - kt \quad (S1)$$

where c_t the solution concentration at time t , C_0 the concentration at the start of the experiment, t the reaction time, and k the first-order rate constant of the DMT.

b. *Pseudo-first order,*

$$\ln \left(\frac{q_e - q_t}{q_e} \right) = -k_1 t \quad (\text{S2})$$

where q_e and q_t are adsorption capacity (mg/g) at equilibrium and at any time t and k_1 pseudo first order rate constant (h^{-1})

c. *Pseudo second order,*

$$\frac{t}{q_t} = \frac{1}{k_2 q_e^2} + \frac{t}{q_e} (\text{S3})$$

where q_t and q_e have the same meaning as above and k_2 (g/mg. h) rate constant for Pseudo-second order.

d. *Modified Elovich model,*

$$X_s = a_s + b_s \ln t \quad (\text{S4})$$

X_s is the amount of sorbate at time t , a_s is the intercept which depends on the type of sorbent and independent of sorbate and b_s the slope which is the function of sorbent and sorbate and may be considered as the rate constant.³

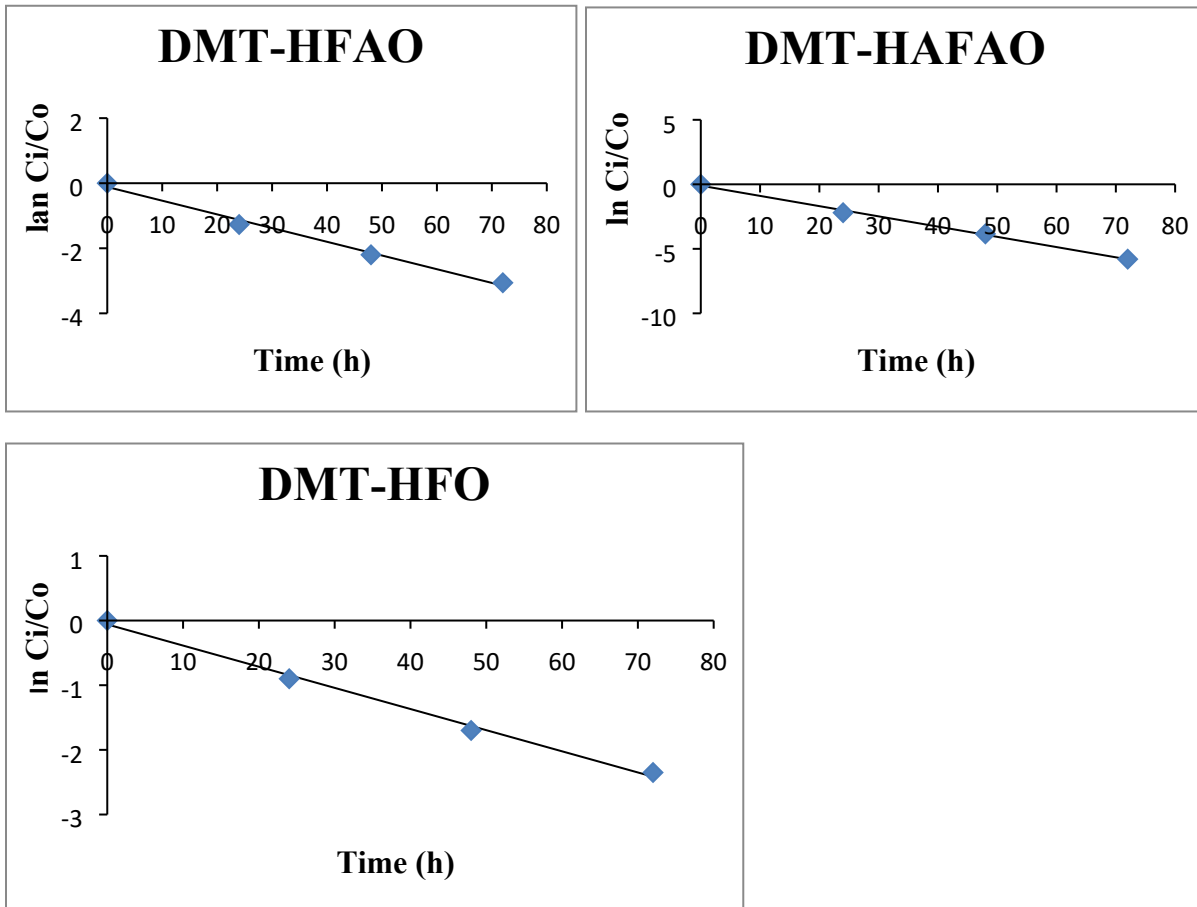
e. *Intra-particle diffusion model*

$$q_t = K_p t^{0.5} + C \quad (\text{S5})$$

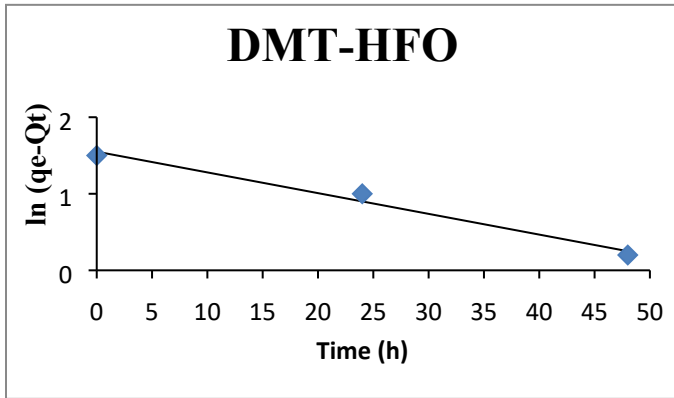
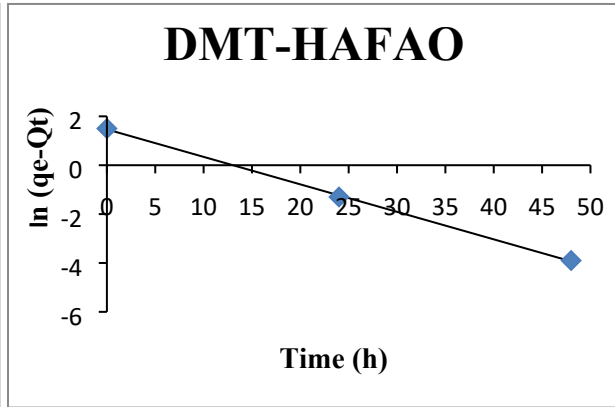
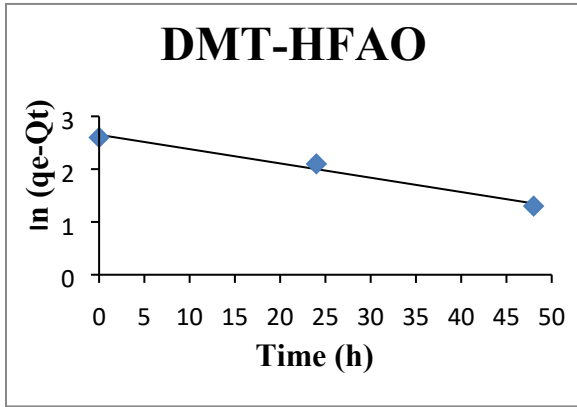
where q_t is the adsorption capacity (milligrams of P per gram of the adsorbent at time t) and K_p is the intra-particle diffusion rate constant and C is a constant gained from the intercept of plot of q_t against $t^{0.5}$.

For equations 3-7 $\ln \frac{C_t}{C_o}$, $\ln \left(\frac{q_e - q_t}{q_t} \right)$ and $\frac{t}{q_t}$ against time t ; X_s against $\ln t$ and q_t against $t^{0.5}$ were plotted.

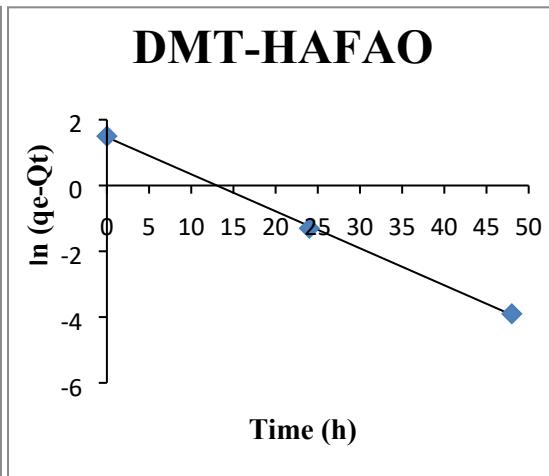
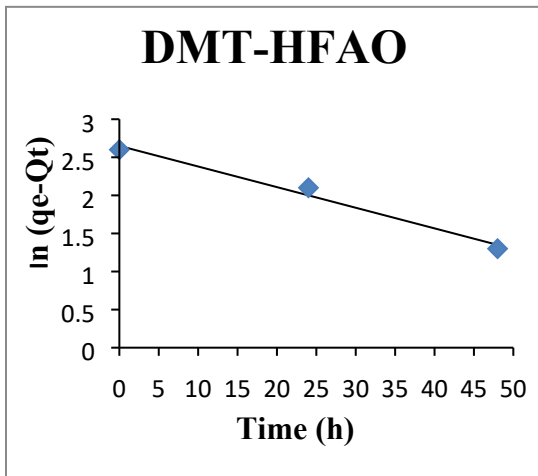
First order rate law



Pseudo first order model



Pseudo second order model



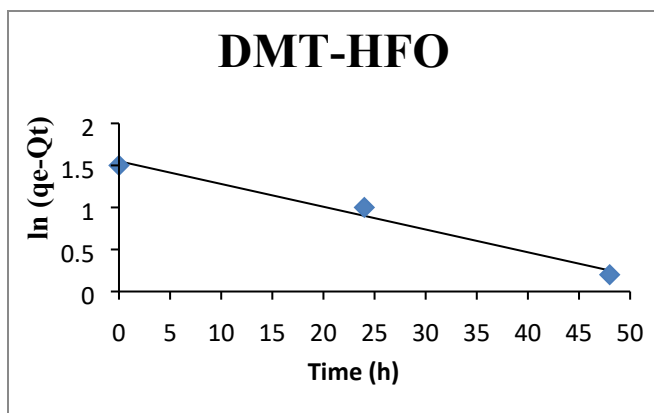


Figure S4: Kinetic models fitted to experimental data generated by DMT-HFO, DMT HFAO and DMT-HAFAO

The coefficient of determination, and related parameters (Table S3, Figure S3) revealed the fitness in the following order: DMT-HFAO: First order \approx pseudo first order > Elovich > Pseudo second order; DMT-HAFAO: pseudo first order (50, 100 ppm) > pseudo second order > Elovich > first order; DMT-HFO: pseudo first order > first order > Elovich > pseudo second order. The high applicability of pseudo first order and Elovich of present kinetic data to the new mode of application in this study is in agreement with previous studies of sorption of phosphates on synthesized sorbents.^{1,4,5}

First order and second order models

As shown in Table S3 and Figure S3, the coefficient of determination (R^2) indicated that the first order model was most suitable in describing the kinetic data for DMT-HFAO and DMT-HFO than DMT-HAFAO. The value of first order rate constant, k , for DMT-HAFAO was higher than the value of DMT-HFAO and DMT-HFO perhaps due to leakage of HAFAO through membrane

Table S3: DMT-sorbent data fitness to kinetic models and related parameters

Kinetics Models							
First order				Pseudo first order			
R ²	k(h ⁻¹)	R ²	k ₁ (h ⁻¹)	q _e (mg/g)			
DMT-HFAO	0.983-0.998	0.046±0.01	0.982-0.993	0.027-0.031	6.89-37.85		
DMT-HAFAO	0.951-0.977	0.068±0.03	0.892-0.999	0.052-0.112	2.2-13		
DMT-HFO	0.987-0.994	0.028±0.02	0.954-0.998	0.027-0.045	1.59-8.87		
Pseudo second order				Elovich			
R ²	k ₂ (g/mg.h)	q _e (mg/g)	h _o mg/g.h	R ²	b(mg/g.h)	a _s (mg/g)	
DMT-HFAO	0.768-0.857	0.0091-0.002	7.1-40	0.57-3.2	0.932-0.989	1.62	9.7
DMT-HAFAO	0.772-0.999	0.32-0.008	3-11.5	0.47-6.7	0.205-0.457	-	-
DMT-HFO	0.286-0.874	0.01	1.94- 9	0.81	0.929-0.984	0.91	7.2
Intra-particle diffusion model							
DMT-sorbent-ppm P	R ²			Kp			
DMT-HFAO-10	0.996			0.115			
DMT-HFAO-30	0.973			1.439			
DMT-HFAO-50	0.981			1.614			
DMT-HFAO-100	0.964			3.238			
DMT-HFO-10	0.986			0.063			
DMT-HFO-30	0.971			0.165			
DMT-HFO-50	0.960			0.403			
DMT-HFO-100	0.995			0.660			
DMT-HAFAO-10	0.534			0.337			
DMT-HAFAO-30	0.533			0.392			
DMT-HAFAO-50	0.987			0.112			
DMT-HAFAO-100	0.999			0.382			

and hence low diffusion resistance.¹The k value for our system, DMT-HFAO, was higher ($0.046 \pm 0.01 \text{ h}^{-1}$) than k value of the reference HFO–DMT ($k = 0.028 \pm 0.01 \text{ h}^{-1}$), which could be attributed to variation in the sorption capacities of the sorbents. This is consonant with the parameter ‘ b ’ considered in Elovich kinetic model which revealed higher b value for DMT-HFAO than DMT-HFO (Table S3). The sorption data also fitted very well to pseudo first order model for DMT-HFAO as evidenced by higher coefficient of determination (Table S3). The rate constant for pseudo first order (k_1) was higher in DMT-HFAO and DMT-HFO than DMT-HFAO. The possible leakage noted in the case of HFAO might have resulted to some of the active sorbent adhered on the external surface of the DMT creating a direct contact with the P from soil solution.

As the coefficient of determination indicates (Table S3), pseudo second order model generally fits fairly well the binary systems. In sharp contrast, very poor correlation was exhibited by the single reference system in particular at lower phosphate concentration. The rate constant for pseudo second order (k_2) exhibited higher values in DMT-HFAO and DMT-HFO than DMT-HFAO. The initial rate for pseudo second order, h_0 , increased with increasing initial concentration, while pseudo second order rate constant k_2 decreased, which could be due to site saturation. Tofik *et al.* (2016)⁶ reported that the kinetic data fitted better to pseudo second order than pseudo first order by direct contact of nano-sized Al-Fe mixed oxide with initial concentration of 20 ppm phosphate solution. Same authors found pseudo second order rate constant, k_2 and equilibrium adsorption capacity, q_e to be 0.36 g/mg.h and 5.025 mg/g respectively. Their report is closer to our report for the amorphous sorbent, which are 0.31 g/mg.h and 4.6 mg/g for 30 ppm P solution. The slight difference may be due to concentration

difference and amorphous nature of the sorbent. Thus the potential of DMT-HAFAO to adsorb phosphate still sounds good in spite of its leakage through dialysis membrane, making it a potential candidate in different mode of application provided that the leakage is managed. However, the report for nano-sized Fe-Al mixed oxide sorbent is not consistent (Tofiket *al.*, 2016)⁶ with our report of the same sorbent. The reason for this inconsistency is due to mode of application of the sorbents in dialysis membrane tube, which in our case slows down the sorption process.⁷

Elovich and Intra-particle diffusion Models

The data generated by DMT-HFAO and DMT-HFO fitted very well to Elovich model, where as data obtained from DMT-HAFAO fitted poorly (Table S3). The model revealed higher a_s (9.7 mg/g) and b (1.62 mg/g.h) values for DMT-HAFO than DMT-HFO. This indicated chemisorption on the sorbent HAFO being more dominant than HFO. Ruan and Gilkes (1996)³ reported a_s values in the range 6.92-15.46 mg/g and b values varying from 0.74 to 2.05 mg/g.h for 0% and 30% alumina composited goethite treated at different temperatures for the concentration of 20 and 40 ppm of phosphate solution.

Data fitness to intra-particle diffusion model is summarized in Table S3 for the range of concentrations studied and the results obtained exhibits the following order: DMT-HFAO ($R^2=0.964-0.996$) > DMT-HFO ($R^2=0.960-0.995$) > DMT-HAFAO ($R^2=0.534-0.999$). The plot of q_t versus $t^{1/2}$ (Figure S3a) for DMT-HFAO illustrates bilinear trends revealing the presence of two or more pathways in the sorption process.^{4,8} The bilinear trend reveals two or more involved mechanisms. The first linear portion was a fast stage. This could be due to the relatively quick transfer of phosphate anions from bulk phase to particle surface as the adsorption was conducted

in a well-agitated system. This is followed by intra-particle diffusion in macro, meso and micro pores. The slope of the second portion represents the rate constant corresponding to intra-particle diffusion.^{9,10} The intra-particle diffusion rate constant, k_p was higher for DMT-HFAO than DMT-HFO and increased with increasing initial phosphate concentrations in both cases. Contrary to this trend, DMT-HAFAO showed no consistent increase due to leakage of HAFAO through membrane. The kinetic data did not also fit the intra-particle model for 10 and 30 ppm phosphate solution. The rate of phosphate transfer in the first linear portion was quicker for 50 and 100 ppm concentrations and resulted in lower intra-particle diffusion (Figure S4).

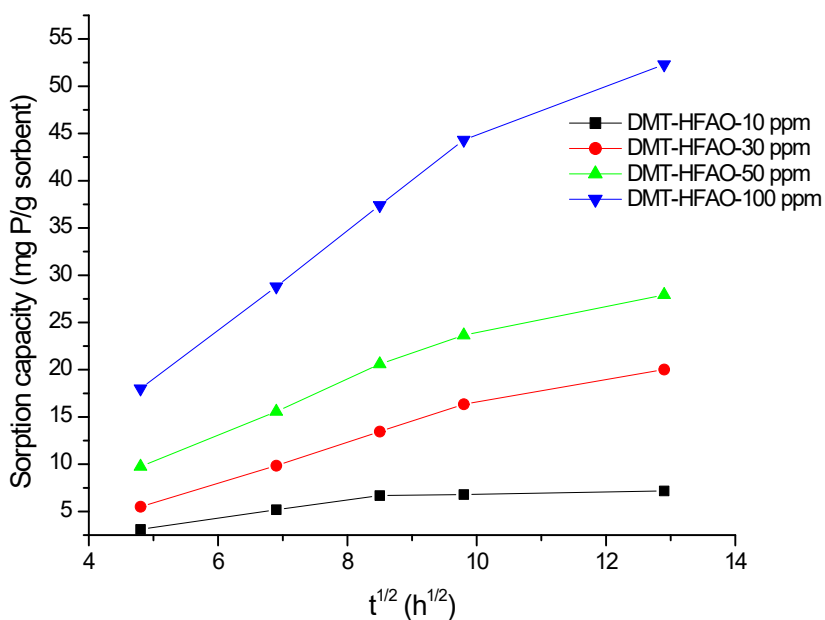


Figure S5: Sorption kinetics of DMT-HFAO fitting to intra-particle model for the studied range of concentrations

It is, therefore, justifiable to further investigate the potential of amorphous sorbent, Fe-Al mixed oxide, by devising a mechanism to suppress the leakage since its sorption capacity for phosphate

in dialysis membrane has been good.¹¹The higher rate constant indicated that intra-particle diffusion is more dominant in the case of DMT-HFAO. In fact, intra-particle diffusion model provides a more comprehensive view of sorption as a series of distinct steps.¹²

Table S4: DMT-sorbent-soil data fitness to intra-particle diffusion model and diffusion rate for Gununo and Bishoftu soils

Intra-particle diffusion model				
Gununo			Bishoftu	
	R ²	k _p (mg/g.h ^{0.5})	R ²	k _p (mg/g.h ^{0.5})
DMT-HFAO	0.980	7.31	0.992	11.98
DMT-HAFAO	0.781	1.45	0.806	3.89
DMT-HFO	0.986	1.40	0.992	2.98

Table S4 shows the coefficients of determination and rate constant values for the three DMT-sorbent-systems based on intra-particle diffusion model. For both Bishoftu and Gununo soils, the intra-particle diffusion rate constant, k_p was higher for DMT-HFAO than DMT-HAFAO and DMT-HFO because of its higher sorption capacity. This indicated higher pore diffusion possibility when sorption is high and this finding is consonant with report by Biswas *et al.* (2007)¹³. For Bishoftu soil, k_p was higher for DMT-HAFAO than DMT-HFO in spite of the fact that it fitted the linear portion less ($R^2=0.806$). This is supposed to be due to sorption of P by DMT-HAFAO from rapidly desorbable pool of Bishoftu soil that avails more P in soil solution (Figure 5a). In this case, the effect of leaked HAFAO is less pronounced as P in solution is relatively high for such soil with low P fixing capacity. However, DMT-HFAO-Bi has higher k_p may be due to surface modification (Ochwohet *et al.*, 2015)¹⁴ compared to DMT-HAFAO-Bi, it desorbed more P from rapid and slow pools. The fact that k_p for DMT-HFAO-Gn was lower than

DMT-HFAO-Bi (Table S4) reflects more P was sorbed in the intra-particle diffusion mode which can be from labile and slow labile P pool of Bishoftu soil. This is in agreement with the cumulative amounts of P desorbed from Gununo and Bishoftu soils (figure S9b).

The sorption data generated from DMT-HAFAO-Bi ($R^2= 0.869$) and DMT-HAFAO-Gn ($R^2= 0.864$) fit to first order kinetics model well (Figure S9c). The corresponding rate constants for pool A of these soils were 0.01917 h^{-1} and 0.01604 h^{-1} for Bishoftu and Gununo soils respectively. This again indicated that the effect of HAFAO leakage through membrane is more pronounced when P releasing ability of the soil is low in the case of Gununo site soil. The trend shown by DMT-HAFAO observed in the case of pure phosphate solution was also observed in the case of soil extracts. As one could discern from Figure 6, in the intervals of 24-48 h, DMT-HAFAO-Gn and DMT-HAFAO-Bi extracted less amount of P due to leakage of the sorbent material. The decreased amount of P in aqueous solution retarded it to satisfy sorption of P on HAFAO inside the membrane. This resulted in quantitative loss of P that might have been detected if it had been adsorbed internally. Even for the intervals between 72-96 h of extraction, the change in cumulative P sorption on DMT-HAFAO was gradual for both Bishoftu (pH=6.8) and Gununo (pH=3.52) soils. This prevented HAFAO in this study to be a potential P scavenger inside membrane tube (2.5-5 nm) for P extraction. Despite this fact, HAFAO could be a promising potential candidate when used in membranes with pore size $< 2.5 \text{ nm}$ provided that the entrance of phosphate ions via such small pores is not affected.^{2,15}

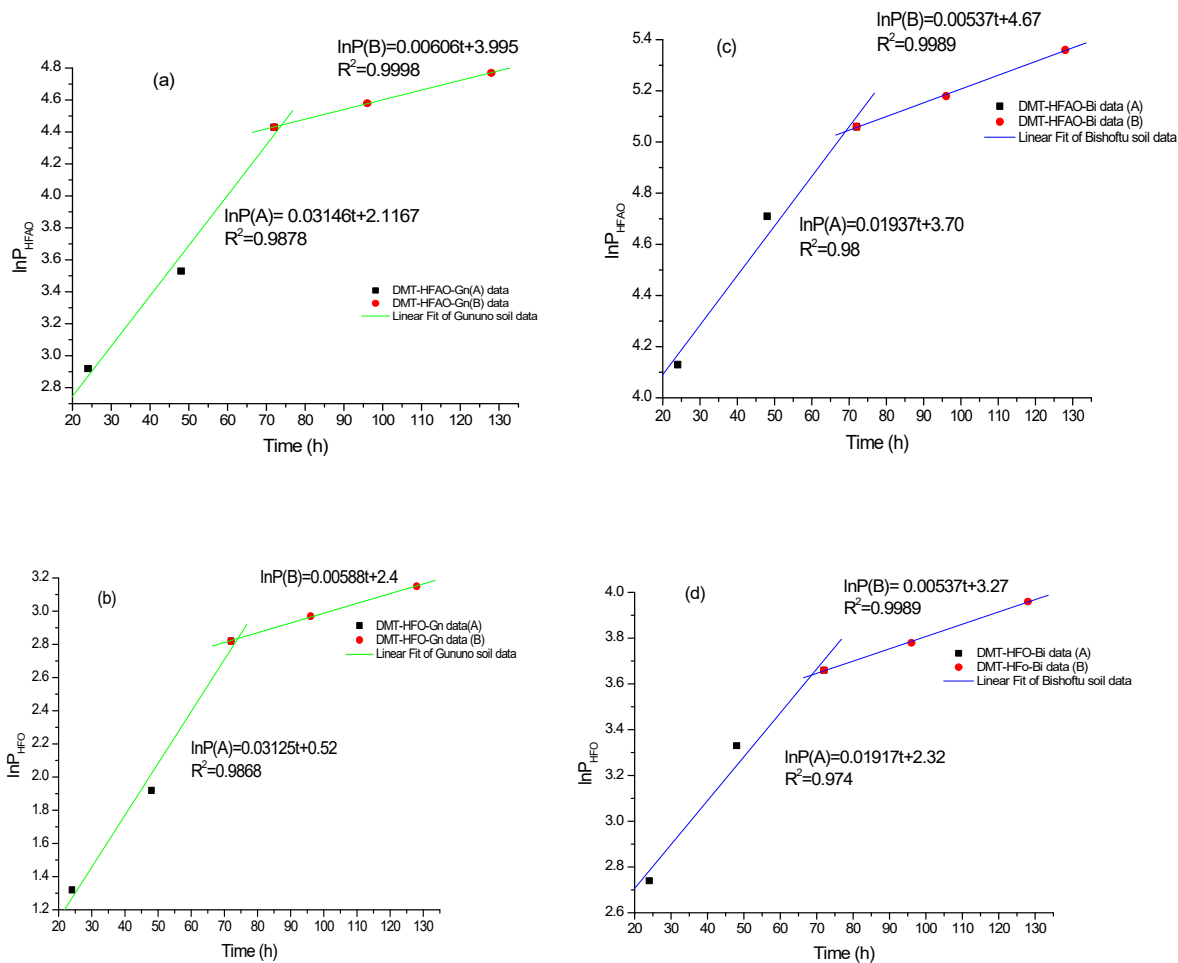


Figure S6: The natural logarithm of phosphate release from Gununo and Bishoftu soil.

Table S5: Quantitative test data for CPS and APS leakage through DMT.

(Control = deionized $H_2O + H_2SO_4$)

Time (h)	Control	Absorbance		mg/L	
		CPS (HFAO)	APS (HFAO)	CPS (HFAO)	APS (HFAO)
12	0.000	0.001	0.003	0.023	0.078
16	0.000	0.000	0.005	0.000	0.130
20	0.000	0.000	0.008	0.000	0.208
24	0.000	-0.006	0.01	0.000	0.260

References

- 1 D. Freese, R. Lookman, R. Merckx and W. H. Riemsdijk, *Soil Sci.Soc.Am.J.*, 1995,**59**, 1295-1300.
- 2V. M. Belousov, V.M., Chertov, E. V. Rozhkova, V. I. Litvin, V.I. and V. A. Zazhigalov, *Theor. Exp. Chem*, 1997, **33**, 103-105.
- 3H. D. Ruan and R. J. Gilkes, *Clay Miner.*,1996, **31**, 63-74.
- 4B. Abebe, A. M. Taddesse, I. Diaz., T. Kebede and E. Teju, *Environ. Chem. Eng.*, 2017, **5**, 1330-1340.
- 5T. Liu, K. Wu, and L. Zeng, *J. Hazard. Mater.*, 2012, **217-218**, 29-35.
- 6 A.S. Tofik, A. M. Taddesse, K.T. Tesfahun and G.G. Girma, *J. Environ. Chem. Eng.*, 2016, **4**, 2458-2468.
- 7 E. Frossard, L. M. Condrón, A. Oberson, S. Sinaj and J. C. Fardeau, J. C., *J. Environ. Qual.*,2000, **29**,15-23.
- 8 A. Zeeshan, M. Atif, U. Muhammad, K. Simon, L. Jiabin, D. Renjie and W. Shubiao, *J. Colloid Interface Sci.*, 2018, **528**, 145–155.
- 9 J. Lalley, H. Changseok, L. Xuan, D. D. Dionysios and N. N. Mallikarjuna, *Chem. Eng. J.*, 2016**284**, 1386–1396.
- 10Z. Ren, L. Shao and G. Zhang, *Water Air SoilPollut*, 2012, **223**, 4221-4231.
- 11A. F. De Sousa, T. P. Braga, Chagas, E. C. Gomes, A. Valentini and E. Longhinotti, *Chem. Eng. J.*, 2012, **210**, 143-149.
- 12 M. D'Arcy, D. Weiss, M. Bluck and R. Vilar, *J.Colloid Interface Sci.*, 2011, **364**, 205-212.
- 13 K. Biswas, S. K. Saha and U. C. Ghosh, *Ind. Eng. Chem. Res.*, 2007,**46**, 5346-5356.
- 14 V. A. Ochwoh, A. S. Claassense and P. C. de Jager, *Commun Soil Sci Plant Anal.*, 2005, **36**,535-556.
- 15X. Wang, F. Liu, W. Tan, W. Li, X. Fengand D. L. Sparks,*SoilSci.*, 2013**178**, 1-11.